Bifurcation analysis of predator-prey model with Cosner type functional response and combined harvesting

Biruk Tafesse Mulugeta [1,2], Jingli Ren[1], Qigang Yuan [3], Liping Yu[4*]

[1] Henan Academy of Big data, Zhengzhou University, Zhengzhou, China

[2] Department of Mathematics, Dilla University, Dilla, Ethiopia

[3] School of Mathematics and Statistics, North China University of Water Resources and Electric Power, Zhengzhou, China

[4] College of Science, Henan University of Technology, Zhengzhou, China

Abstract

In this paper, we consider a predator-prey model with Cosner type functional response and combined harvesting. First, we explore the existence and stability of the equilibria. Then using the center manifold theorem and normal form theory, we investigate codimension one and codimension two bifurcations of the model. The analysis shows that the system has a variety of bifurcation phenomena including transcritical bifurcation, saddle-node bifurcation, Hopf bifurcation, Bogdanov-Takens bifurcation and homoclinic bifurcation. Our findings indicate that the dynamics with harvesting are significantly richer than the system without harvesting. Finally, numerical simulations are provided to support the analytical results.

Keywords:
Predator-prey model, Cosner type functional response, Harvesting, Stability, Bifurcations

*Corresponding author:lpyu@haut.edu.cn

1 Introduction

Since the first differential equation model proposed by Lotka [1] and Volterra [2], numerous predator-prey models have been studied. The prototype predator-prey model is of the form

$$\begin{cases} \dfrac{dN}{dT} = f(N)N - g(N,P)P, \\ \dfrac{dP}{dT} = \epsilon g(N,P)P - \mu P, \end{cases} \tag{1}$$

where N and P are population densities of prey and predator species respectively. $f(N)$ is the net growth rate of the prey in the absence of predators and $g(N,P)$ is the consumption rate of a predator to prey. The positive constants ϵ and μ represent the conversion rate of the captured prey into the predator and the predator death rate respectively. The behavioral characteristic of the predator species can be reflected by the element $g(N,P)$ called functional response or trophic function. Many scholars have investigated population dynamics using different types of functional responses, such as Holling type II [3], Holling type III [4, 5], Beddington-DeAngelis [6], ratio-dependent [7, 8], Sigmoidal [5], Monod-Holdane [4, 9, 10] and the like. However, concerning cooperative hunting in predator-prey models, there are few functional responses. Taking into consideration how group of predators search, contact and hunt a herd of prey, and making different biological assumptions, Cosner et al. [11] presented the following functional response

$$g(N,P) = \frac{Ce_0NP}{1+hCe_0NP}, \tag{2}$$

where C, h and e_0 are the amount of prey captured by a predator per encounter, handling time per prey and the total encounter coefficient between the predator and the prey respectively. They are all assumed to be positive. Combining the functional response (2) and logistic prey growth rate, Ryu et al. [12] proposed the following predator-prey model and studied it qualitatively

$$\begin{cases} \dfrac{dN}{dT} = rN(1-\dfrac{N}{K}) - \dfrac{Ce_0NP}{1+hCe_0NP}p, \\ \dfrac{dP}{dT} = \dfrac{\epsilon Ce_0NP}{1+hCe_0NP}P - \mu P. \end{cases} \tag{3}$$

They investigated the occurrence of saddle-node bifurcation, Hopf bifurcation and Bogdanov-Takens bifurcation, and observed bi-stability behavior in the coexistence and predator-free equilibrium points. Incorporating double Allee effect on the growth function of the prey in system (3), Tiwari et. al [13] analyzed the dynamical behaviors of the resulting system.

From the ecological point of view, harvesting of predator species had been given much emphasis to control the predator species and prevent prey species from extinction. As a result, many scholars investigated the dynamic of predator-prey model with a harvesting term in both the prey and predator growth equations, such as constant harvesting [14, 15], proportional harvesting [16, 17, 18] and nonlinear harvesting [19, 20, 21, 22, 23, 24, 25]. But all those only consider the comonly known functional responses. Literatures on the effect of harvesting on the dynamics of predator-prey interaction with the functional response (2) are very few in number. Recently, to avoid the extreme phenomena leading to the eventual extinction of predators as a result of too weak cooperation of predators, Shang et al [26] added constant yield prey harvesting H on system (3) and investigated the arrangement of renewable resources

$$\begin{cases} \dfrac{dN}{dT} = rN(1-\dfrac{N}{K}) - \dfrac{Ce_0NP}{1+hCe_0NP}P + H, \\ \dfrac{dP}{dT} = \dfrac{\epsilon Ce_0NP}{1+hCe_0NP}P - \mu P. \end{cases} \tag{4}$$

They obtained different conditions for the existence and stability of equilibria, and investigated repelling and attracting Bogdanov–Takens bifurcations by perturbing two bifurcation parameters near the cusp point. However, continuous harvesting of only prey species at a constant rate independent of density will result in insufficient food for predators as a result of over-exploitation, then both species may be extinct with elapse of time. Besides, for ecological balance and healthy economic development, we should consider not only the harvesting of prey species but also predator species. Proportional harvesting, which depends on the harvested density, is more realistic than the constant harvesting. Therefore, we apply proportional harvesting to system (3) to explore the dynamics of a predator-prey model with cooperative hunting and combined proportional harvesting.

The paper is organized as follows. In Sec. 2, the mathematical model is formulated. In Sec. 3, boundedness of solutions, the existence and types of equilibria are discussed. In Sec. 4, local and global bifurcations around different equilibrium points are studied. To illustrate the analytical results, numerical simulations are carried out in Sec. 5. Finally, the conclusion is presented in Sec. 6.

2 The mathematical model

Incorporating combined harvesting, system (3) becomes

$$\begin{cases} \dfrac{dN}{dT} = rN(1-\dfrac{N}{K}) - \dfrac{Ce_0NP}{1+hCe_0NP}P - q_1EN, \\ \dfrac{dP}{dT} = \dfrac{\epsilon Ce_0NP}{1+hCe_0NP}P - \mu P - q_2EP, \end{cases} \tag{5}$$

where q_i $(i=1,2)$ and E are the catchability coefficients of prey and predator species and harvesting effort respectively. Using the following scale

$$x = \frac{N}{K}, \quad y = Khe_0CP, \quad \alpha_1 = \frac{1}{rCe_0(hK)^2}, \quad t = rT, \quad \alpha_2 = \frac{\epsilon}{rh}, \quad h_1 = \frac{q_1E}{r},$$
$$h_2 = \frac{q_2E}{r}, \quad \text{and} \quad \gamma = \frac{\mu}{r},$$

we obtain the form

$$\begin{cases} \dfrac{dx}{dt} = x(1-x) - \dfrac{\alpha_1 xy^2}{1+xy} - h_1x, \\ \dfrac{dy}{dt} = \dfrac{\alpha_2 xy^2}{1+xy} - (\gamma + h_2)y. \end{cases} \tag{6}$$

3 Boundedness, existence and types of equilibria

3.1 Boundedness

Lemma 3.1. *All solutions of system (6) are bounded in* $\Omega = \{(x,y) : x \geq 0, y \geq 0\}$.

Proof. Let $(x(t), y(t))$ be any solution of system (6) with non negative initial condition. Denote $\eta(t) = x(t) + \dfrac{\alpha_1}{\alpha_2}y(t)$, then

$$\begin{aligned} \frac{d\eta}{dt} &= \frac{dx}{dt} + \frac{\alpha_1}{\alpha_2}\frac{dy}{dt}, \\ &= x(1-x) - h_1x - \frac{\alpha_1}{\alpha_2}(h_2+\gamma)y, \\ &= -h_1x - \frac{\alpha_1}{\alpha_2}(h_2+\gamma)y + x - x^2. \end{aligned}$$

Let $\theta = min\{h_1, h_2+\gamma\}$, we have

$$\frac{d\eta}{dt} \leq -\theta(x + \frac{\alpha_1}{\alpha_2}y) + 1 - (x - \frac{1}{2})^2,$$

$$= \quad -\theta(x + \frac{\alpha_1}{\alpha_2}y) + 1.$$

Therefore, $\frac{d\eta}{dt} + \theta\eta \leq 1$. Applying the theory of differential inequality, we obtain $0 < \eta(t) < \frac{1 - e^{-\theta t}}{\theta} + \eta(0)e^{-\theta t}$. For $t \to \infty$, $0 < \eta < \frac{1}{\theta}$. This implies the solutions of system (6) are bounded. □

3.2 Existence of equilibria

In this section, we discuss the existence of equilibria for system (6). It is clear that $O(0,0)$ and $E_0(1-h_1, 0)$ (for $h_1 < 1$) are boundary equilibrium points (see Figure 1). The interior equilibrium points are the intersection points of the following equations in the first quadrant

$$\frac{\alpha_1 y^2}{1 + xy} = 1 - h_1 - x, \tag{7a}$$

$$y = \frac{\gamma + h_2}{(\alpha_2 - \gamma - h_2)x}. \tag{7b}$$

If $\alpha_2 > \gamma + h_2$, the denominator of equation (7b) is positive. Substituting equation (7b) in equation (7a), we get a polynomial equation

$$p(x) = A_3x^3 + A_2x^2 + A_0 = 0, \tag{8}$$

where $A_0 = (\gamma + h_2)^2\alpha_1$, $A_2 = (1 - h_1)(h_2 + \gamma - \alpha_2)\alpha_2$ and $A_3 = (\alpha_2 - \gamma - h_2)\alpha_2$. It can be obtained that $x = 0$ and $x = \frac{2}{3}(1 - h_1)$ are possible extreme points of the polynomial equation (8). Then we have the following lemma.

Lemma 3.2. *Suppose $h_1 < 1$ and $h_2 < \alpha_2 - \gamma$.*

(i) If $\alpha_1(\gamma + h_2)^2 > \frac{4}{27}\alpha_2(1 - h_1)^3(\alpha_2 - \gamma - h_2)$, then system (6) has no interior equilibrium points (see Figure 2) ;

(ii) If $\alpha_1(\gamma + h_2)^2 = \frac{4}{27}\alpha_2(1 - h_1)^3(\alpha_2 - \gamma - h_2)$, then system (6) has a unique interior equilibrium point $E^*(x^*, y^*) = E^*\left(\frac{2}{3}(1-h_1), \frac{3(\gamma + h_2)}{2(1 - h_1)(\alpha_2 - \gamma - h_2)}\right)$ (see Figure 3);

(iii) If $\alpha_1(\gamma+h_2)^2 < \frac{4}{27}\alpha_2(1-h_1)^3(\alpha_2-\gamma-h_2)$*, then system* (6) *has two distinict interior equilibrium points* $E_1(x_1, y_1)$ *and* $E_2(x_2, y_2)$*, where* $0 < x_1 < \frac{2}{3}(1-h_1) < x_2 < 1$ *(see Figure 4).*

Proof. It is clear that $p''(x) = 6A_3x+2A_2$. Here $p''(0) = -2\alpha_2(1-h_1)(\alpha_2-\gamma-h_2) < 0$ and $p''(\frac{2}{3}(1-h_1)) = 2(1-h_1)(\alpha_2-\gamma-h_2)\alpha_2 > 0$, so the polynomial $p(x)$ in (8) has local maximum $\alpha_1(\gamma+h_2)^2$ and local minimum $(\gamma+h_2)^2\alpha_1 - \frac{4}{27}\alpha_2(1-h_1)^3(\alpha_2-\gamma-h_2)$ at $x = 0$ and $x = \frac{2}{3}(1-h_1)$ respectively.

(i) If $\alpha_1(\gamma+h_2)^2 > \frac{4}{27}\alpha_2(1-h_1)^3(\alpha_2-\gamma-h_2)$, the graph of the polynomial (8) never crosses x-axis for $x > 0$ and system (6) has no interior equlibrium.

(ii) If $\alpha_1(\gamma+h_2)^2 = \frac{4}{27}\alpha_2(1-h_1)^3(\alpha_2-\gamma-h_2)$, $p(\frac{2}{3}(1-h_1)) = 0$ and the graph of the polynomial $p(x)$ touches x-axis only at $x = \frac{2}{3}(1-h_1)$. This means that the system has a unique interior equilibrium point $E^*(x^*, y^*) = E^*\left(\frac{2}{3}(1-h_1), \frac{3(\gamma+h_2)}{2(1-h_1)(\alpha_2-\gamma-h_2)}\right)$.

(iii) If $\alpha_1(\gamma+h_2)^2 < \frac{4}{27}\alpha_2(1-h_1)^3(\alpha_2-\gamma-h_2)$, $p(\frac{2}{3}(1-h_1)) < 0$, its graph crosses x-axis at two points for $x > 0$ and system (6) has two distinct interior equlibria $E_1(x_1, y_1)$ and $E_2(x_2, y_2)$.

□

3.3 Types of equilibrium points

In this section, we discuss the local stability of equilibrium points. The Jacobian matrix of system (6) at any equlibrium $E(x, y)$ is given by

$$J(E(x,y)) = \begin{pmatrix} 1-h_1-2x-\dfrac{\alpha_1 y^2}{(1+xy)^2} & \dfrac{-\alpha_1 xy(2+xy)}{(1+xy)^2} \\ \dfrac{\alpha_2 y^2}{(1+xy)^2} & -h_2-\gamma+\dfrac{\alpha_2 xy(2+xy)}{(1+xy)^2} \end{pmatrix}.$$

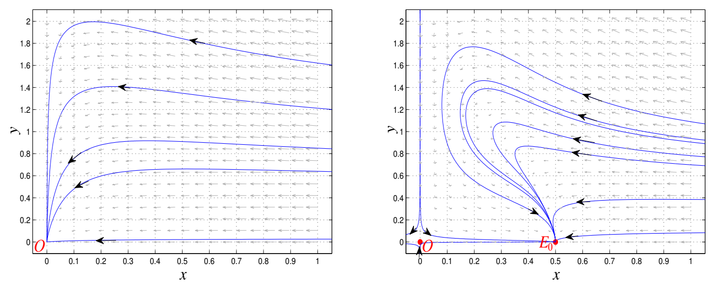

(a) **(b)**

Figure 1: Phase portraits of boundary equlibria for system (6) at $\alpha_1 = 0.3$, $\alpha_2 = 0.9$, $h_2 = 0.2$, $\gamma = 0.03$. **(a)** $O(0,0)$ is a stable node for $h_1 = 1.3$. **(b)** $O(0,0)$ is unstable and $E_0(1-h_1,0)$ is stable for $h_1 = 0.5$.

In particular, the Jacobian matrices at two boundary equilibria are

$$J(O(0,0)) = \begin{pmatrix} 1-h_1 & 0 \\ 0 & -h_2-\gamma \end{pmatrix} \text{ and } J(E_0(1-h_1,0)) = \begin{pmatrix} -1+h_1 & 0 \\ 0 & -h_2-\gamma \end{pmatrix}.$$

Lemma 3.3. *The trivial equilibrium point $O(0,0)$ is*

(i) locally asymptotically stable if $h_1 > 1$;

(ii) unstable if $h_1 < 1$:

(iii) nonhyperbolic if $h_1 = 1$.

Lemma 3.4. *$E_0(1-h_1,0)$ is always locally asymptotically stable.*

The phase portrait is shown in Figure 1.

Lemma 3.5. *Suppose $\alpha_1(\gamma+h_2)^2 = \frac{4}{27}\alpha_2(1-h_1)^3(\alpha_2-\gamma-h_2)$. The unique interior equilibrium point $E^*(x^*,y^*) = E^*\left(\frac{2}{3}(1-h_1), \frac{3(h_2+\gamma)}{2(1-h_1)(\alpha_2-h_2-\gamma)}\right)$ is*

(i) saddle-node if $\frac{2}{3}(-1+h_1)+h_2+\gamma-\frac{(h_2+\gamma)(-1+h_1+3h_2+3\gamma)}{3\alpha_2} \neq 0$;

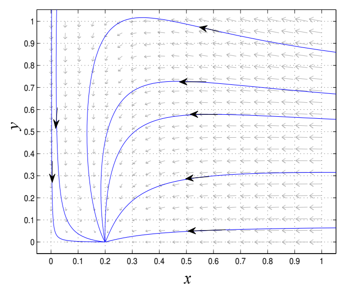

Figure 2: Phase portraits of no interior equilibrium for system (6) under $\alpha_1 = 0.3$, $\alpha_2 = 0.9$, $h_1 = 0.8$, $h_2 = 0.2$, $\gamma = 0.03$.

(ii) a cusp point of codimension 2 if $\frac{2}{3}(-1+h_1)+h_2+\gamma - \frac{(h_2+\gamma)(-1+h_1+3h_2+3\gamma)}{3\alpha_2} = 0.$

The corresponding phase portraits are shown in Figure 3.

Proof. From Lemma 3.2(ii) if $\alpha_1(\gamma+h_2)^2 = \frac{4}{27}\alpha_2(1-h_1)^3(\alpha_2-\gamma-h_2)$, system (6) has a unique interior equilibrium point $E^*(x^*, y^*)$. The Jacobian matrix of system (6) at $E^*(x^*, y^*)$ is

$$J(E(x^*, y^*)) = \begin{pmatrix} -\frac{(-1+h_1)(h_2+\gamma-2\alpha_2)}{3\alpha_2} & \frac{4(-1+h_1)^3(h_2+\gamma-2\alpha_2)(h_2+\gamma-\alpha_2)}{27\alpha_2(h_2+\gamma)} \\ \frac{9(h_2+\gamma)^2}{4\alpha_2(-1+h_1)^2} & -\frac{(h_2+\gamma)(h_2+\gamma-\alpha_2)}{\alpha_2} \end{pmatrix}.$$

The eigenvalues of $J(E^*(x^*, y^*))$ are $\lambda_1 = 0$ and $\lambda_2 = \frac{2}{3}(-1+h_1)+h_2+\gamma - \frac{(h_2+\gamma)(-1+h_1+3h_2+3\gamma)}{3\alpha_2}$, so, $E^*(x^*, y^*) = E^*\left(\frac{2}{3}(1-h_1), \frac{3(h_2+\gamma)}{2(1-h_1)(\alpha_2-h_2-\gamma)}\right)$ is nonhyperbolic. The stability can't be determined by the technique of linearization. Using the translation

$$\begin{cases} x = u + \frac{2}{3}(1-h_1), \\ y = v + \frac{3(h_2+\gamma)}{2(1-h_1)(\alpha_2-h_2-\gamma)}, \end{cases}$$

we bring $E^*(x^*, y^*)$ to the origin and in a new coordinate of u and v, system (6) becomes

$$\begin{cases} \dot{u} = a_{10}u + a_{01}v + a_{20}u^2 + a_{11}uv + a_{02}v^2 + o(|u,v|)^3, \\ \dot{v} = b_{10}u + b_{01}v + b_{20}u^2 + b_{11}uv + b_{02}v^2 + o(|u,v|)^3, \end{cases} \tag{9}$$

where

$$\begin{aligned}
a_{10} &= -\frac{(-1+h_1)(h_2+\gamma-2\alpha_2)}{3\alpha_2},\ a_{01} = \frac{4(-1+h_1)^3(h_2+\gamma-2\alpha_2)(h_2+\gamma-\alpha_2)}{27(h_2+\gamma)\alpha_2}, \\
a_{20} &= -1 - \frac{(h_2+\gamma)(h_2+\gamma-\alpha_2)}{2\alpha_2^2},\ a_{11} = \frac{4(-1+h_1)^2(h_2+\gamma-\alpha)^3}{9(h_2+\gamma)\alpha_2^2}, \\
a_{02} &= -\frac{8(-1+h_1)^4(h_2+\gamma-\alpha_2)^4}{81(h_2+\gamma)^2\alpha_2^2},\ b_{10} = \frac{9(h_2+\gamma)^2}{4(-1+h_1)^2\alpha_2}, \\
b_{01} &= -\frac{(h_2+\gamma)(h_2+\gamma-\alpha_2)}{\alpha_2},\ b_{20} = \frac{27(h_2+\gamma)^3}{8(-1+h_1)^3\alpha_2^2}, \\
b_{11} &= -\frac{3(h_2+\gamma)(h_2+\gamma-\alpha_2)^2}{(-1+h_1)\alpha_2^2},\ b_{02} = \frac{2(-1+h_1)(h_2+\gamma-\alpha_2)^3}{3\alpha_2^2}.
\end{aligned}$$

(i) If $\frac{2}{3}(-1+h_1)+h_2+\gamma-\frac{(h_2+\gamma)(-1+h_1+3h_2+3\gamma)}{3\alpha_2} \neq 0$, $\lambda_2 \neq 0$ and there exists a smooth non-singular transformation. Let $T = \begin{pmatrix} v_1 & v_2 \end{pmatrix} = \begin{pmatrix} 1 & \frac{a_{10}}{b_{10}} \\ -\frac{a_{10}}{a_{01}} & 1 \end{pmatrix}$, using the translation $(u,v)^T = T(x,y)^T$ and introduce a new time variable $\tau = (a_{10}+b_{01})t$, we get

$$\begin{cases} \dot{x} = c_{20}x^2 + c_{11}xy + c_{02}y^2 + o(|x,y|)^3, \\ \dot{y} = y + d_{20}x^2 + d_{11}xy + d_{02}y^2 + o(|x,y|)^3, \end{cases} \tag{10}$$

where

$$c_{20} = -\frac{9(h_2+\gamma)(h_2+\gamma-\alpha_2)}{2(h_2+\gamma)(-1+h_1+3h_2+3\gamma)-2\alpha_2(-2+2h_1+3h_2+3\gamma)} \neq 0,$$

$$d_{20} = -\frac{27(h_2+\gamma)^2\Big((h_2+\gamma)(-1+h_1+3h_2+3\gamma)+\alpha_2(-1+h_1-3h_2-3\gamma)\Big)}{8\alpha_2(-1+h_1)^3\Big(-(h_2+\gamma)(-1+h_1+3h_3+3\gamma)+\alpha_2(-2+2h_1+3h_2+3\gamma)\Big)} \neq 0.$$

Therefore, according to Theorem 7.1 in [27] [Zhang et al., 1992], if $\frac{2}{3}(-1 + h_1) + h_2 + \gamma - \frac{(h_2+\gamma)(-1+h_1+3h_2+3\gamma)}{3\alpha_2} \neq 0$, the equilibrium $E^*(x^*, y^*)$ is a saddle-node.

(ii) If $\frac{2}{3}(-1 + h_1) + h_2 + \gamma - \frac{(h_2+\gamma)(-1+h_1+3h_2+3\gamma)}{3\alpha_2} = 0$, then $\lambda_2 = 0$. Making the following transformation

$$\begin{cases} x = v, \\ y = b_{10}u + b_{01}v, \end{cases}$$

system (9) becomes

$$\begin{cases} \dot{x} = y + \gamma_{20}x^2 + \gamma_{11}xy + \gamma_{02}y^2 + o(|x,y|^2), \\ \dot{y} = s_{20}x^2 + s_{11}xy + s_{02}y^2 + o(|x,y|^2), \end{cases} \tag{11}$$

where

$$\begin{aligned} \gamma_{20} &= -\frac{2(h_2+\gamma)(h_2+\gamma-\alpha_2)^3}{\alpha_2(h_2+\gamma-2\alpha_2)}, \ \gamma_{11} = -\frac{4(h_2+\gamma-\alpha_2)^2}{h_2+\gamma-2\alpha_2}, \\ \gamma_{02} &= -\frac{2(h_2+\gamma-\alpha_2)}{h_2+\gamma-2\alpha_2}, \ s_{20} = -\frac{6(h_2+\gamma)^2(h_2+\gamma-\alpha_2)^4}{\alpha_2(h_2+\gamma-2\alpha_2)^2}, \\ s_{11} &= -\frac{12(h_2+\gamma)(h_2+\gamma-\alpha_2)^3}{(h_2+\gamma-2\alpha_2)^2}, \ s_{02} = -\frac{2(h_2+\gamma-\alpha_2)^2(h_2+\gamma+2\alpha_2)}{(h_2+\gamma-2\alpha_2)^2}. \end{aligned}$$

According to the normal form given in [28], we obtain an equivalent system of (11) as follows

$$\begin{cases} \dot{x} = y, \\ \dot{y} = s_{20}x^2 + (s_{11} + 2\gamma_{20})xy + o(|x,y|^2), \end{cases} \tag{12}$$

where $s_{20} < 0$ and $s_{11} + 2\gamma_{20} = -\frac{4(h_2+\gamma)(h_2+\gamma-\alpha_2)^3(h_2+\gamma+\alpha_2)}{\alpha_2(h_2+\gamma-2\alpha_2)^2} > 0$. So the coefficients of the terms x^2 and xy in system (12) are non zero, by Theorem 3 in [28], E^* is a cusp of codimension 2.

□

Lemma 3.6. *Let* $\alpha_1(\gamma + h_2)^2 < \frac{4}{27}\alpha_2(1-h_1)^3(\alpha_2 - \gamma - h_2)$.

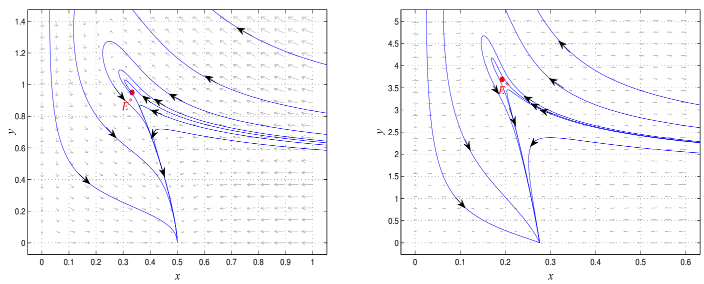

(a) **(b)**

Figure 3: Phase portraits of unique interior equilibrium for system (6). **(a)** $E^*(x^*, y^*)$ is a saddle-node at $\alpha_1 = 0.243133$, $\alpha_2 = 0.997862$, $h_1 = 0.5$, $h_2 = 0.04$, $\gamma = 0.2$. **(b)** $E^*(x^*, y^*)$ is a cusp point at $\alpha_1 = 0.010537$, $\alpha_2 = 0.6$, $h_1 = 0.724167$, $h_2 = 0.0492072$, $\gamma = 0.2$.

(i) $E_1(x_1, y_1)$ *is locally asymptotically stable if one of the following conditions hold.*

(i1) $-1 + h_1 + 2x_1 = 0$ *and* $\dfrac{4\alpha_1(h_2 + \gamma)}{\alpha_2(-1 + h_1)^2} > \alpha_2 - h_2 - \gamma$;

(i2) $-1 + h_1 + 2x_1 < 0$ *and* $\dfrac{(h_2 + \gamma)^2(\alpha_1 + \alpha_2 x_1^2)}{\alpha_2^2 x_1^2} > 1 - h_1 - 2x_1 + h_2 + \gamma$;

(i3) $-1 + h_1 + 2x_1 > 0$, $\dfrac{(h_1 + \gamma)^2(\alpha_1 + \alpha_2 x_1^2)}{\alpha_2^2 x_1} > 1 - h_1 - 2x_1 + h_2 + \gamma$ *and* $(h_2 + \gamma)^2\alpha_1 > \alpha_2 x_1^2(-1 + h_1 + x_1)(\alpha_2 - h_2 - \gamma)$.

(ii) $E_2(x_2, y_2)$ *is always saddle.*

The corresponding phase portraits are shown in Figure 4.

Proof. From Lemma 3.2(iii), if $\alpha_1(\gamma + h_2)^2 < \dfrac{4}{27}\alpha_2(1 - h_1)^3(\alpha_2 - \gamma - h_2)$, system (6) has two distinct interior equilibria $E_1(x_1, y_1)$ and $E_2(x_2, y_2)$ which satisfy
$0 < x_1 < \dfrac{2}{3}(1 - h_1) < x_2 < 1.$

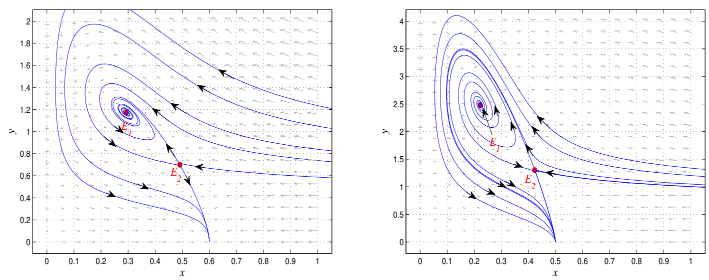

(a) **(b)**

Figure 4: Phase portraits of the two interior equilibria for system (6). **(a)** $E_1(x_1, y_1)$ is a stable focus and $E_2(x_2, y_2)$ is saddle at $\alpha_1 = 0.3$, $\alpha_2 = 0.9$, $h_1 = 0.4$, $h_2 = 0.2$, $\gamma = 0.03$. **(b)** $E_1(x_1, y_1)$ is an unstable focus and $E_2(x_2, y_2)$ is saddle at $\alpha_1 = 0.07$, $\alpha_2 = 0.9$, $h_1 = 0.5$, $h_2 = 0.3$, $\gamma = 0.02$.

(i) The Jacobian matrix of system (6) at $E_1(x_1, y_1)$ is

$$J(E_1(x_1, y_1)) = \begin{pmatrix} 1 - h_1 - 2x_1 - \dfrac{\alpha_1(h_2+\gamma)^2}{\alpha_2^2 x_1^2} & \dfrac{\alpha_1(h_2+\gamma)(h_2+\gamma-2\alpha_2)}{\alpha_2^2} \\ \dfrac{(h_2+\gamma)^2}{\alpha_2 x_1^2} & -\dfrac{(h_2+\gamma)(h_2+\gamma-\alpha_2)}{\alpha_2} \end{pmatrix}$$

and its characteristic equation is $\lambda^2 + A_1\lambda + A_0 = 0$.

(i1) If $-1 + h_1 + 2x_1 = 0$, $x_1 = \dfrac{1-h_1}{2}$ and $y_1 = \dfrac{2(h_2+\gamma)}{(1-h_1)(\alpha_2 - h_2 - \gamma)}$. Then $A_1 = (h_2+\gamma)\left(\dfrac{4\alpha_1(h_2+\gamma)}{\alpha_2^2(-1+h_1)^2} - \dfrac{\alpha_2 - h_2 - \gamma}{\alpha_2}\right)$ and $A_0 = \dfrac{4\alpha_1(h_2+\gamma)^3}{\alpha_2^2(-1+h_1)^2} > 0$. It is clear that if $\dfrac{4\alpha_1(h_2+\gamma)}{\alpha_2(-1+h_1)^2} > \alpha_2 - h_2 - \gamma$, then $A_1 > 0$. Therefore by Routh-Hurwitz criteria $E_1(x_1, y_1)$ is locally asymptotically stable.

(i2) If $-1+h_1+2x_1 < 0$, then $A_1 = -1+h_1+2x_1-h_2-\gamma+\dfrac{(h_2+\gamma)^2(\alpha_1+\alpha_2 x_1^2)}{\alpha_2^2 x_1^2}$ and $A_0 = \dfrac{(h_2+\gamma)\Big((h_2+\gamma)^2\alpha_1 - (\alpha_2 - h_2 - \gamma)(-1+h_1+2x_1)\alpha_2 x_1^2\Big)}{\alpha_2^2 x_1^2} >$

0. $A_1 > 0$ if $\dfrac{(h_2+\gamma)^2(\alpha_1+\alpha_2 x_1^2)}{\alpha_2^2 x_1^2} > 1 - h_1 - 2x_1 + h_2 + \gamma$. $E_1(x_1, y_1)$ is locally asymptotically stable.

(i3) For $-1 + h_1 + 2x_1 > 0$, $A_1 > 0$ if $\dfrac{(h_2+\gamma)^2(\alpha_1+\alpha_2 x_1^2)}{\alpha_2^2 x_1^2} > 1 - h_1 - 2x_1 + h_2 + \gamma$, and $A_0 > 0$ if $(h_2+\gamma)^2\alpha_1 > \alpha_2 x_1^2(-1 + h_1 + x_1)(\alpha_2 - h_2 - \gamma)$. Therefore $E_1(x_1, y_1)$ is locally asymptotically stable.

(ii) From $\dfrac{2}{3}(1 - h_1) < x_2$, we have $-1 + h_1 + 2x_2 > 0$. The characteristic equation of the Jacobian matrix at $E_2(x_2, y_2)$ is

$$\lambda^2 + A_1\lambda + A_0 = 0,$$

where $A_1 = -1 + h_1 + 2x_2 - h_2 - \gamma + \dfrac{(h_2+\gamma)^2(\alpha_1+\alpha_2 x_2^2)}{\alpha_2^2 x_2^2}$ and $A_0 = \dfrac{(h_2+\gamma)\Big((h_2+\gamma)^2\alpha_1 - (\alpha_2 - h_2 - \gamma)(-1 + h_1 + 2x_2)\alpha_2 x_2^2\Big)}{\alpha_2^2 x_2^2}$. Since $(\gamma + h_2)^2\alpha_1 < \dfrac{4}{27}\alpha_2(1 - h_1)^3(\alpha_2 - \gamma - h_2)$, $A_0 < 0$. Therefore $E_2(x_2, y_2)$ is always saddle.

□

4 Bifurcation analysis

4.1 Codimension one bifurcations

In this section, we investigate the existence of codimension one bifurcations at different equilibrium points with respect to different parameters.

Transcritical bifurcation

Theorem 4.1. *If $h_1 = h_1^{TC} = 1$, system (6) undergoes transcritical bifurcation at $O(0, 0)$.*

The proof is simple, so we omit it here.

Saddle-node bifurcation

Theorem 4.2. *If* $h_1 = h_1^{SN} = 1 - 2x_1 + \dfrac{\alpha_1(h_2+\gamma)^2}{\alpha_2 x_1^2(\alpha_2 - h_2 - \gamma)}$ *and* $\alpha_1(h_2+\gamma)(h_2+\gamma-2\alpha_2) + \alpha_2 x_1^2(h_2+\gamma-\alpha_2)^2 \neq 0$, *system* (6) *undergoes saddle-node bifurcation at* $E_1(x_1, y_1)$.

Proof. If $h_1 = 1-2x_1 + \dfrac{\alpha_1(h_2+\gamma)^2}{\alpha_2 x_1^2(\alpha_2 - h_2 - \gamma)}$ and $\alpha_1(h_2+\gamma)(h_2+\gamma-2\alpha_2)+\alpha_2 x_1^2(h_2+\gamma-\alpha_2)^2 \neq 0$, one can get that the eigenvalues of the Jacobian matrix at $E_1(x_1, y_1)$ are $\lambda_1 = 0$ and
$\lambda_2 = \dfrac{(h_2+\gamma)\Big(\alpha_1(h_2+\gamma)(h_2+\gamma-2\alpha_2)+\alpha_2 x_1^2(h_2+\gamma-\alpha_2)^2\Big)}{\alpha_2^2 x_1^2(\alpha_2-h_2-\gamma)} \neq 0$. The corresponding eigenvectors are $v_1 = \begin{pmatrix} c \\ 1 \end{pmatrix}$ and $v_2 = \begin{pmatrix} d \\ 1 \end{pmatrix}$, where $c = \dfrac{x_1^2(h_2+\gamma-\alpha_2)}{h_2+\gamma}$ and $d = -\dfrac{\alpha_1(h_2+\gamma-2\alpha_2)}{\alpha_2(h_2+\gamma-\alpha_2)}$.

Let us derive the normal form on center manifold. Using the translation

$$\begin{cases} x = u + x_1, \\ y = v + \dfrac{h_2+\gamma}{x_1(\alpha_2-h_2-\gamma)}, \end{cases}$$

we bring $E_1(x_1, y_1)$ to the origin and in a new coordinate of u and v, the Taylor expansion of system (6) around the origin is

$$\begin{cases} \dot{u} = a_{10}u + a_{01}v + a_{20}u^2 + a_{11}uv + a_{02}v^2 + a_{30}u^3 + a_{03}v^3 \\ \qquad + a_{21}u^2v + a_{12}uv^2 + o(|u,v|)^4, \\ \dot{v} = b_{10}u + b_{01}v + b_{20}u^2 + b_{11}uv + b_{02}v^2 + b_{30}u^3 + b_{03}v^3 \\ \qquad + b_{21}u^2v + b_{12}uv^2 + o(|u,v|)^4, \end{cases} \tag{13}$$

where

$$\begin{aligned} a_{10} &= 1 - h_1 - 2x_1 - \frac{\alpha_1(h_2+\gamma)^2}{\alpha_2^2 x_1^2},\ a_{01} = \frac{\alpha_1(h_2+\gamma)(h_2+\gamma-2\alpha_2)}{\alpha_2^2}, \\ a_{20} &= -1 + \frac{\alpha_1(h_2+\gamma)^3}{\alpha_2^3 x_1^3},\ a_{11} = -\frac{2\alpha_1(h_2+\gamma)(h_2+\gamma-\alpha_2)^2}{\alpha_2^3 x_1}, \\ a_{02} &= \frac{\alpha_1 x_1(h_2+\gamma-\alpha_2)^3}{\alpha_2^3},\ a_{21} = \frac{3\alpha_1(h_2+\gamma)^2(h_2+\gamma-\alpha_2)^2}{\alpha_2^4 x_1^2}, \end{aligned}$$

$$
\begin{aligned}
a_{30} &= -\frac{\alpha_1(h_2+\gamma)^4}{\alpha_2^4x_1^4},\ a_{03}=\frac{\alpha_1x_1^2(h_2+\gamma-\alpha_2)^4}{\alpha_2^4} \\
a_{12} &= -\frac{\alpha_1(h_2+\gamma-\alpha_2)^3(3h_2+3\gamma-\alpha_2)}{\alpha_2^4},\ b_{10}=\frac{(h_2+\gamma)^2}{\alpha_2x_1^2}, \\
b_{01} &= -\frac{(h_2+\gamma)(h_2+\gamma-\alpha_2)}{\alpha_2},\ b_{20}=-\frac{(h_2+\gamma)^3}{\alpha_2^2x_1^3},\ b_{11}=\frac{2(h_2+\gamma)(h_2+\gamma-\alpha_2)^2}{\alpha_2^2x_1}, \\
b_{02} &= -\frac{x_1(h_2+\gamma-\alpha_2)^3}{\alpha_2^2}\ ,b_{30}=\frac{(h_2+\gamma)^4}{\alpha_2^3x_1^4},\ b_{03}=-\frac{x_1^2(h_2+\gamma-\alpha_2)^4}{\alpha_2^3}, \\
b_{21} &= -\frac{3(h_2+\gamma)^2(h_2+\gamma-\alpha_2)^2}{\alpha_2^3x_1^2},\ b_{12}=\frac{(h_2+\gamma-\alpha_2)^3(3h_2+3\gamma-\alpha_2)}{\alpha_2^3}.
\end{aligned}
$$

Let $T=\begin{pmatrix}v_1 & v_2\end{pmatrix}$. Using the translation $\begin{pmatrix}u & v\end{pmatrix}^T=T\begin{pmatrix}x & y\end{pmatrix}^T$, system (13) becomes

$$
\begin{cases}
\dot{x}=c_{20}x^2+c_{11}xy+c_{02}y^2+o(|x,y|)^3, \\
\dot{y}=\lambda y+d_{20}x^2+d_{11}xy+d_{02}y^2+o(|x,y|)^3,
\end{cases}
\tag{14}
$$

where

$$
\begin{aligned}
c_{20}=&\frac{x_1(h_2+\gamma-\alpha_2)^2\Big(\alpha_1(h_2+\gamma)^2+\alpha_2x_1^3(\alpha_2-h_2-\gamma)\Big)}{(h_2+\gamma)\Big(\alpha_1(h_2+\gamma)(h_2+\gamma-2\alpha_2)+\alpha_2x_1^2(h_2+\gamma-\alpha_2)^2\Big)}, \\
d_{20}=&\frac{x_1(h_2+\gamma-\alpha_2)^3\Big(\alpha_2x_1^2\Big(-(h_2+\gamma)^2+\alpha_2(h_2+\gamma+x_1)\Big)-\alpha_1(h_2+\gamma)^2\Big)}{\alpha_2(h_2+\gamma)\Big(\alpha_1(h_2+\gamma)(h_2+\gamma-2\alpha_2)-\alpha_2x_1^2(h_2+\gamma-\alpha_2)^2\Big)}.
\end{aligned}
$$

Here, we do not present other coefficients of system (14) for the complexity.

The local center manifold of system (14) near the origin is

$$
y=-\frac{d_{20}}{\lambda}x^2+o(x^2).
$$

On this one dimensional center manifold, system (14) is reduced into

$$
\dot{x}=c_{20}x^2+o(x^2).
$$

Since $c_{20}\neq 0$ for $\alpha_1(h_2+\gamma)(h_2+\gamma-2\alpha_2)+\alpha_2x_1^2(h_2+\gamma-\alpha_2)^2\neq 0$, then system (6) undergoes saddle-node bifurcation at $E_1(x_1,y_1)$. $\square$

Similarly if we choose h_2, α_1 and α_2 as bifurcation parameters, system (6) also undergoes saddle-node bifurcation at $E_1(x_1, y_1)$.

Theorem 4.3. *If* $h_1 = 1 + \dfrac{3}{\sqrt[3]{4}} \dfrac{\alpha_1\alpha_2(\alpha_2 - h_2 - \gamma)(h_2+\gamma)^4}{\left(\alpha_1\alpha_2^2(h_2+\gamma-\alpha_2)^2(h_2+\gamma)^5\right)^{\frac{2}{3}}}$, *system (6) undergoes saddle-node bifurcation at* $E^*(x^*, y^*)$.

The proof is similar to the proof of Theorem 4.2, so we omit it here.

Hopf bifurcation

Theorem 4.4. *System (6) undergoes Hopf bifurcation at* $E_1(x_1, y_1) = \left(\dfrac{1-h_1}{2}, \dfrac{2(h_2+\gamma)}{(1-h_1)(\alpha_2-h_2-\gamma)}\right)$ *with respect to bifurcation parameter* h_2 *at* $h_2 = h_2^* = \dfrac{-4\alpha_1\gamma + \alpha_2(\alpha_2-\gamma)(-1+h_1)^2}{4\alpha_1 + \alpha_2(-1+h_1)^2}$.

Proof. The eigenvalues of the Jacobian matrix at $E_1(x_1, y_1)$ is

$$\lambda_{1,2} = \frac{T(h_2)}{2} \pm \frac{\sqrt{(T(h_2))^2 - 4\omega^2(h_2)}}{2},$$

where $T(h_2) = (h_2+\gamma)\left(\dfrac{4\alpha_1(h_2+\gamma)}{\alpha_2^2(-1+h_1)^2} + \dfrac{h_2+\gamma-\alpha_2}{\alpha_2}\right)$ and $\omega^2(h_2) = \dfrac{4\alpha_1(h_2+\gamma)^3}{\alpha_2^2(-1+h_1)^2}$.
If $h_2 = h_2^* = \dfrac{-4\alpha_1\gamma + \alpha_2(\alpha_2-\gamma)(-1+h_1)^2}{4\alpha_1+\alpha_2(-1+h_1)^2}$, then $T(h_2^*) = 0$ and $\omega^2(h_2^*) = \dfrac{4\alpha_1\alpha_2^4(-1+h_1)^4}{(4\alpha_1+\alpha_2(-1+h_1)^2)^3}$. The eigenvalues of system (6) at $E_1(x_1, y_1)$ are $\lambda_{1,2} = \pm i\omega(h_2^*)$, where i is an imaginary unit and $\omega(h_2^*) > 0$. To verify the transversality condition, let $\chi = \dfrac{T(h_2)}{2}$. One can show that

$$\frac{d}{dh_2}(\chi)|_{h_2=h_2^*} = \frac{T'(h_2^*)}{2} = 1 \neq 0.$$

Hence, system (6) undergoes Hopf bifurcation at $E_1(x_1, y_1)$. To determine genericity conditions, we compute the first Lyapunov coefficient $l_1(0)$. Using the transformation

$$\begin{cases} x = u + \dfrac{1-h_1}{2}, \\ y = v + \dfrac{2(h_2+\gamma)}{(1-h_1)(\alpha_2-h_2-\gamma)}, \end{cases}$$

we bring $E_1(x_1, y_1)$ to the origin and the Taylor expansion of system (6) around the origin is given by

$$\begin{cases} \dot{u} = m_{10}u + m_{01}v + m_{20}u^2 + m_{11}uv + m_{02}v^2 + m_{30}v^3 + m_{03}v^3 \\ \qquad + m_{21}u^2v + m_{12}uv^2 + o(|u, v|)^4, \\ \dot{v} = n_{10}u + n_{01}v + n_{20}u^2 + n_{11}uv + n_{02}v^2 + n_{30}v^3 \\ \qquad + n_{03}v^3 + n_{21}u^2v + n_{12}uv^2 + o(|u, v|)^4, \end{cases} \tag{15}$$

where

$$\begin{aligned}
m_{10} &= -\frac{4\alpha_1(h_2+\gamma)^2}{\alpha_2^2(-1+h_1)^2},\ m_{01} = \frac{\alpha_1(h_2+\gamma)(h_2+\gamma-2\alpha_2)}{\alpha_2}, \\
m_{11} &= \frac{4\alpha_1(h_2+\gamma)(h_2+\gamma-\alpha_2)^2}{\alpha_2^3(-1+h_1)},\ m_{20} = -1 - \frac{8\alpha_1(h_2+\gamma)^3}{\alpha_2^3(-1+h_1)^3}, \\
m_{02} &= -\frac{\alpha_1(-1+h_1)(h_2+\gamma-\alpha_2)^3}{2\alpha_2^3},\ m_{21} = \frac{12\alpha_1(h_2+\gamma)^2(h_2+\gamma-\alpha_2)^2}{\alpha_2^4(-1+h_1)^2}, \\
m_{12} &= -\frac{\alpha_1(h_2+\gamma-\alpha_2)^3(3h_2+3\gamma-\alpha_2)}{\alpha_2^4},\ m_{30} = -\frac{16\alpha_1(h_2+\alpha_2)^4}{\alpha_2^4(-1+h_1)^4}, \\
m_{03} &= \frac{\alpha_1(-1+h_1)^2(h_2+\gamma-\alpha_2)^4}{4\alpha_2^4},\ n_{10} = \frac{4(h_2+\gamma)^2}{\alpha_2(-1+h_1)^2}, \\
n_{01} &= -\frac{(h_2+\gamma-\alpha_2)(h_2+\gamma)}{\alpha_2},\ n_{11} = -\frac{4(h_2+\gamma)(h_2+\gamma-\alpha_2)^2}{\alpha_2^2(-1+h_1)}, \\
n_{20} &= \frac{8(h_2+\gamma)^3}{\alpha_2^2(-1+h_1)^3},\ n_{02} = \frac{(-1+h_1)(h_2+\gamma-\alpha_2)^3}{2\alpha_2^2}, \\
n_{12} &= \frac{(h_2+\gamma-\alpha_2)^3(3h_2+3\gamma-\alpha_2)}{\alpha_2^3},\ n_{21} = -\frac{12(h_2+\gamma)^2(h_2+\gamma-\alpha_2)^2}{\alpha_2^3(-1+h_1)^2}, \\
n_{30} &= \frac{16(h_2+\gamma)^4}{\alpha_2^3(-1+h_1)^4},\ n_{03} = -\frac{(-1+h_1)^2(h_2+\gamma-\alpha_2)^4}{4\alpha_2^3}.
\end{aligned}$$

Suppose U_1+iU_2 be the eigenvector corresponding to the eigenvalue $\lambda = i\omega$, where U_1 and U_2 are real vectors. By simple calculation, we obtain $U_1 = \begin{pmatrix} n \\ 1 \end{pmatrix}$ and $U_2 = \begin{pmatrix} \frac{\omega}{s} \\ 0 \end{pmatrix}$, where $n = -\frac{\alpha_1}{\alpha_2}$ and $s = \frac{4\alpha_2^3(-1+h_1)^2}{(4\alpha_1+\alpha_2(-1+h_1)^2)^2}$. Let $p = \begin{pmatrix} U_1 & U_2 \end{pmatrix} = \begin{pmatrix} n & \frac{\omega}{s} \\ 1 & 0 \end{pmatrix}$, and using the transformation $\begin{pmatrix} u & v \end{pmatrix}^T = p \begin{pmatrix} x & y \end{pmatrix}^T$, we obtain the following normal form

$$\begin{cases} \dot{x} =& \omega y + \alpha_{11}xy + \alpha_{20}x^2 + \alpha_{02}y^2 + \alpha_{30}x^3 \\ & + \alpha_{03}y^3 + \alpha_{21}x^2y + \alpha_{12}xy^2 + O(|x,y|^4), \\ \dot{y} =& -\omega x + b_{11}xy + b_{20}x^2 + b_{02}y^2 + b_{30}x^3 \\ & + b_{03}y^3 + b_{21}x^2y + b_{12}xy^2 + O(|x,y|^4), \end{cases} \tag{16}$$

where $\alpha_{ij}, b_{ij}(i,j = 1,2,3)$ are coefficients of system (16) and we choose not to present here. The first Lyapunov coefficient l_1 is computed using the formula in [28]

$$\begin{aligned} l_1 =& \frac{3\pi}{2\omega}\bigg[3(\alpha_{30} + b_{03}) + (\alpha_{12} + b_{21}) - \frac{2}{\omega}(\alpha_{20}b_{20} - \alpha_{02}b_{02}) - \frac{\alpha_{11}}{\omega}(\alpha_{02} + b_{20}) \\ & + \frac{b_{11}}{\omega}(b_{02} + b_{20})\bigg]. \end{aligned}$$

Here due to complexity of $l_1(0)$, we cannot determine its sign or whether it vanishes. Generally we have the following conclusions.

1. If $l_1 < 0$, the system undergoes supercritical Hopf bifurcation;
2. If $l_1 > 0$, the system undergoes subcritical Hopf bifurcation;
3. If $l_1 = 0$, the system undergoes degenerate Hopf bifurcation.

□

Theorem 4.5. *If* $h_1 = h_1^* = 1 - 2x_1 + h_2 + \gamma - \dfrac{(h_2+\gamma)^2(\alpha_1 + \alpha_2 x_1^2)}{\alpha_2^2 x_1^2}$ *and* $\alpha_1(h_2+\gamma)(2\alpha_2 - h_2 - \gamma) > \alpha_2 x_1^2(\alpha_2 - h_2 - \gamma)^2$*, system* (6) *undergoes Hopf bifurcation at* $E_1(x_1, y_1)$.

Theorem 4.6. *If* $\alpha_1 = \alpha_1^* = \alpha_2 x_1^2\bigg(-1 + \dfrac{\alpha_2(1 - h_1 + h_2 + \gamma - 2x_1)}{(h_2+\gamma)^2}\bigg)$ *and* $\dfrac{\alpha_2(2 - 2h_1 + h_2 + \gamma - 4x_1)}{h_2 + \gamma} > (1 - h_1 + h_2 + \gamma + 2x_1)$*, then system* (6) *undergoes Hopf bifurcation at* $E_1(x_1, y_1)$.

The proofs of Theorem 4.5 and 4.6 are similar to the proof of Theorem 4.4, so we omit them here. Moreover, if we choice α_2 as bifurcation parameter, system (6) also undergoes Hopf bifurcation at $E_1(x_1, y_1)$.

4.2 Codimension two bifurcation

Bogdanov-Takens bifurcation

In this subsection, we investigate the existence of codimension two bifurcation. From Lemma 3.2(ii) and Lemma 3.5, system (6) has a unique interior equilibrium $E^*(x^*, y^*)$ which is a cusp point of codimension 2, for $\alpha_1(\gamma+h_2)^2 = \frac{4}{27}\alpha_2(1-h_1)^3(\alpha_2-\gamma-h_2)$ and $\frac{2}{3}(-1+h_1)+h_2+\gamma-\frac{(h_2+\gamma)(-1+h_1+3h_2+3\gamma)}{3\alpha_2}=0$. In the following theorem, choosing rational parameters, we illustrate the occurrence of Bogdanov-Takens bifurcation at $E^*(x^*, y^*)$ under a small parameter perturbation.

Theorem 4.7. *If α_2 and h_2 are chosen as bifurcation parameters, system (6) undergoes Bogdanov-Takens bifurcation of codimension 2 in a small neighborhood at E^* as (α_2, h_2) varies near $(\alpha_2^{[BT]}, h_2^{[BT]})$, where $(\alpha_2^{[BT]}, h_2^{[BT]})$ is the threshold value of bifurcation parameters satisfying*
$Det(J(E^*))|_{(\alpha_2,h_2)=(\alpha_2^{[BT]},h_2^{[BT]})}=0$ and $Tr(J(E^*))|_{(\alpha_2,h_2)=(\alpha_2^{[BT]},h_2^{[BT]})}=0$.

Proof. To derive the normal form of Bogdanov-Takens bifurcation for system (6), and obtain the analytical expressions for saddle-node bifurcation, Hopf bifurcation and homoclinic bifurcation curves in a small neighborhood of BT point, we consider the following perturbed system

$$\begin{cases} \dfrac{dx}{dt} = x(1-x) - \dfrac{\alpha_1 xy^2}{1+xy} - h_1 x, \\ \dfrac{dy}{dt} = \dfrac{(\alpha_2^{[BT]}+\xi_1)xy^2}{1+xy} - \gamma y - (h_2^{[BT]}+\xi_2)y, \end{cases} \tag{17}$$

where $\xi = (\xi_1, \xi_2)$ is a parameter vector in a small neighborhood of $(0,0)$. Using the translation

$$\begin{cases} x = u + \dfrac{2}{3}(1-h_1), \\ y = v + \dfrac{3(h_2^{[BT]}+\gamma)}{2(1-h_1)(\alpha_2^{[BT]}-h_2^{[BT]}-\gamma)}, \end{cases}$$

E^* is brought to the origin and the Taylor expansion of the resulting system is

$$\begin{cases} \dot{u} = a_{10}u + a_{01}v + a_{20}u^2 + a_{11}uv + a_{02}v^2 + P_1(u,v,\xi), \\ \dot{v} = b_{00} + b_{10}u + b_{01}v + b_{20}u^2 + b_{11}uv + b_{02}v^2 + Q_1(u,v,\xi), \end{cases} \tag{18}$$

where $P_1(u,v,\xi)$ and $Q_1(u,v,\xi)$ are high order smooth functions of (u,v) and the coefficients depend smoothly on ξ_1 and ξ_2,

$$
\begin{aligned}
a_{10} &= \frac{(1-h_1)(h_2^{[BT]}+\gamma-2\alpha_2^{[BT]})}{3\alpha_2^{[BT]}},\ a_{20}=-1-\frac{(h_2^{[BT]}+\gamma)(h_2^{[BT]}+\gamma-\alpha_2^{[BT]})}{2(\alpha_2^{[BT]})^2},\\
a_{01} &= \frac{4(-1+h_1)^3(h_2^{[BT]}+\gamma-2\alpha_2^{[BT]})(h_2^{[BT]}+\gamma-\alpha_2^{[BT]})}{27(h_2^{[BT]}+\gamma)\alpha_2^{[BT]}},\\
a_{11} &= \frac{4(-1+h_1)^2(h_2^{[BT]}+\gamma-\alpha_2^{[BT]})^3}{9(h_2^{[BT]}+\gamma)(\alpha_2^{[BT]})^2},\ a_{02}=-\frac{8(-1+h_1)^4(h_2^{[BT]}+\gamma-\alpha_2)^4}{81(h_2^{[BT]}+\gamma)^2(\alpha_2^{[BT]})^2},\\
b_{00} &= \frac{3(h_2^{[BT]}+\gamma)(h_2^{[BT]}+\gamma)\xi_1-\alpha_2^{[BT]}\xi_2)}{2(-1+h_1)(h_2^{[BT]}+\gamma-\alpha_2^{[BT]})\alpha_2^{[BT]}},\ b_{10}=\frac{9(h_2^{[BT]}+\gamma)^2(\alpha_2^{[BT]}+\xi_1)}{4(-1+h_1)(\alpha_2^{[BT]})^2},\\
b_{01} &= \frac{(h_2^{[BT]}+\gamma)\Big(\alpha_2^{[BT]}(-h_2^{[BT]}-\gamma+2\xi_1)-(h_2^{[BT]}+\gamma)\xi_1\Big)}{(\alpha_2^{[BT]})^2}+h_2^{[BT]}+\gamma-\xi_2,\\
b_{20} &= \frac{27(h_2^{[BT]}+\gamma)^3(\alpha_2^{[BT]}+\xi_1)}{8(-1+h_1)^3(\alpha_2^{[BT]})^3},\ b_{11}=-\frac{3(h_2^{[BT]}+\gamma)(h_2^{[BT]}+\gamma-\alpha_2^{[BT]})^2(\alpha_2^{[BT]}+\xi_1)}{(-1+h_1)(\alpha_2^{[BT]})^3},\\
b_{02} &= \frac{2(-1+h_1)(h_2^{[BT]}+\gamma-\alpha_2^{[BT]})^3(\alpha_2^{[BT]}+\xi_1)}{3(\alpha_2^{[BT]})^3}.
\end{aligned}
$$

Making affine transformation

$$
\begin{cases} x=u,\\ y=a_{10}u+a_{01}v,\end{cases}
$$

we get

$$
\begin{cases} \dot{x}=y+r_{20}x^2+r_{02}y^2+P_2(x,y,\xi),\\ \dot{y}=s_{00}+s_{10}x+s_{01}y+s_{20}x^2+s_{02}y^2+Q_2(x,y,\xi),\end{cases} \tag{19}
$$

where $P_2(x,y,\xi)$ and $Q_2(x,y,\xi)$ are high order smooth functions of (x,y) and the coefficients depend smoothly on ξ_1 and ξ_2

$$
\begin{aligned}
r_{20} &= \frac{a_{10}(a_{02}a_{10}-a_{01}a_{11})}{a_{01}^2}+a_{20},\ r_{02}=\frac{a_{02}}{a_{01}^2},\ s_{00}=a_{01}b_{00},\ s_{10}=-a_{10}b_{01}+a_{01}b_{10},\\
s_{01} &= a_{10}+b_{01},\ s_{20}=\frac{a_{02}a_{10}^3+b_{20}a_{01}^3+a_{01}a_{10}\Big(a_{10}(b_{02}-a_{11})+a_{01}(a_{20}-b_{11})\Big)}{a_{01}^2},\\
s_{02} &= \frac{a_{02}a_{10}+a_{01}b_{02}}{a_{01}^2}.
\end{aligned}
$$

Under c^∞ change of coordinates in a small neighborhood of $(0,0)$

$$\begin{cases} x_1 = x - \dfrac{s_{02}}{2}x^2 - r_{02}xy, \\ y_1 = y + r_{20}x^2 - s_{02}xy, \end{cases}$$

system (19) becomes

$$\begin{cases} \dot{x_1} = \gamma_{10}x_1 + \gamma_{01}y_1 + \gamma_{20}x_1^2 + \gamma_{11}x_1y_1 + P_3(x_1, y_1, \xi), \\ \dot{y_1} = \eta_{00} + \eta_{10}x_1 + \eta_{01}y_1 + \eta_{20}x_1^2 + \eta_{11}x_1y_1 + Q_3(x_1, y_1, \xi), \end{cases} \tag{20}$$

where $P_3(x_1, y_1, \xi)$ and $Q_3(x_1, y_1, \xi)$ are high order smooth functions of (x_1, y_1) and the coefficients depend smoothly on ξ_1 and ξ_2,

$$\begin{aligned} \gamma_{10} =& - r_{02}s_{00},\ \gamma_{01} = 1,\ \gamma_{11} = -r_{02}(r_{02}s_{00} + s_{01}),\ \gamma_{20} = -\frac{1}{2}r_{02}\Bigg(s_{00}s_{02} + 2s_{10}\Bigg), \\ \eta_{00} =& s_{00},\ \eta_{10} = -s_{00}s_{02} + s_{10},\ \eta_{01} = s_{01},\ \eta_{11} = r_{02}(2 - s_{00}s_{02} + s_{10}), \\ \eta_{20} =& - r_{20}s_{01} - \frac{1}{2}s_{02}\Bigg(s_{00}s_{02} + s_{10}\Bigg) + s_{20}. \end{aligned}$$

Again under c^∞ change of coordinates in a small neighborhood of $(0,0)$

$$\begin{cases} u = x_1 - \dfrac{\gamma_{11}}{2\gamma_{01}}x_1^2, \\ v = y_1 - \left(\dfrac{\gamma_{10}\gamma_{11}}{2\gamma_{01}^2} - \dfrac{\gamma_{20}}{\gamma_{01}}\right)x_1^2, \end{cases}$$

system (20) can be transformed as

$$\begin{cases} \dot{u} = \alpha_{10}u + \alpha_{01}v + P_4(u, v, \xi), \\ \dot{v} = \beta_{00} + \beta_{10}u + \beta_{01}v + \beta_{20}u^2 + \beta_{11}uv + Q_4(u, v, \xi), \end{cases} \tag{21}$$

where $P_4(u, v, \xi)$ and $Q_4(u, v, \xi)$ are high order smooth functions of (u, v) and the coefficients depend smoothly on ξ_1 and ξ_2,

$$\begin{aligned} \alpha_{10} =& \gamma_{10},\ \alpha_{01} = \gamma_{01},\ \beta_{00} = \eta_{00},\ \beta_{10} = \eta_{10},\ \beta_{01} = \eta_{01},\ \beta_{11} = -\frac{\gamma_{10}\gamma_{11}}{\gamma_{01}} + 2\gamma_{20} + \eta_{11}, \\ \beta_{20} =& \eta_{20} + \frac{\gamma_{01}(4\gamma_{10}\gamma_{20} + \eta_{01}(\gamma_{11} - 2\gamma_{20})) + \gamma_{10}\gamma_{11}(\eta_{01} - 2\gamma_{10})}{2\gamma_{01}^2}. \end{aligned}$$

Let

$$\begin{cases} x = u, \\ y = \alpha_{10}u + \alpha_{01}v + P_4(u, v, \xi), \end{cases}$$

then system (21) becomes

$$\begin{cases} \dot{x} = y, \\ \dot{y} = c_0 + c_1 x + c_2 y + c_3 x^2 + c_4 xy + Q_5(x, y, \xi), \end{cases} \tag{22}$$

where $Q_5(x, y, \xi)$ is high order smooth function of (x, y) and the coefficients depend smoothly on ξ_1 and ξ_2,

$$\begin{aligned} c_0 =& \alpha_{01}\beta_{00},\ c_1 = \alpha_{01}\beta_{10} - \alpha_{10}\beta_{01},\ c_2 = \alpha_{10} + \beta_{01},\ c_3 = \alpha_{01}\beta_{20} - \alpha_{10}\beta_{11}, \\ c_4 =& \beta_{11}. \end{aligned}$$

Due to the complexity of the expression of c_3, it is difficult to determine its sign. Therefore, we consider the following two cases.

Case 1: If $c_3 > 0$, for small ξ_1 and ξ_2, we make the following transformation

$$X = x,\ Y = \frac{y}{\sqrt{c_3}},\ \tau = \sqrt{c_3}t.$$

System (22) turns into

$$\begin{cases} \dot{X} = Y, \\ \dot{Y} = \dfrac{c_0}{c_3} + \dfrac{c_1}{c_3}X + \dfrac{c_2}{\sqrt{c_3}}Y + X^2 + \dfrac{c_4}{\sqrt{c_3}}XY + Q_6(X, Y, \xi), \end{cases} \tag{23}$$

where $Q_6(X, Y, \xi)$ is high order smooth function of (X, Y) and the coefficients depend smoothly on ξ_1 and ξ_2. To annihilate the term X of the second equation for system (23), taking

$$u = X + \frac{c_1}{2c_3}, v = Y,$$

system (23) can be changed as

$$\begin{cases} \dot{u} = v, \\ \dot{v} = \left(\dfrac{c_0}{c_3} - \dfrac{c_1^2}{4c_3^2}\right) + \left(\dfrac{c_2}{\sqrt{c_3}} - \dfrac{c_1 c_4}{2c_3\sqrt{c_3}}\right)v + u^2 + \dfrac{c_4}{\sqrt{c_3}}uv + Q_7(u, v, \xi), \end{cases} \tag{24}$$

where $Q_7(u, v, \xi)$ is high order smooth functions of (u, v) and the coefficients depend smoothly on ξ_1 and ξ_2. Suppose that $\beta_{11}(\xi_1, \xi_2) \neq 0$ for small ξ_1 and ξ_2, $\dfrac{c_4}{\sqrt{c_3}} \neq 0$, using change of coordinates

$$x = \frac{c_4^2}{c_3}u,\ y = \frac{c_4^3}{c_3\sqrt{c_3}}v,\ \tau = \frac{\sqrt{c_3}}{c_4}t,$$

we obtain the versal unfolding of perturbed system (17)

$$\begin{cases} \dot{x} = y, \\ \dot{y} = \mu_1(\xi_1, \xi_2) + \mu_2(\xi_1, \xi_2)y + x^2 + xy + Q_8(x, y, \xi), \end{cases} \tag{25}$$

where

$$\mu_1(\xi_1, \xi_2) = \left(c_0 - \frac{c_1^2}{4c_3}\right)\frac{c_4^4}{c_3^3}, \ \mu_2(\xi_1, \xi_2) = \left(c_2 - \frac{c_1 c_4}{2c_3}\right)\frac{c_4}{c_3}, \tag{26}$$

and $Q_8(x, y, \xi)$ is high order smooth functions of (x, y) and the coefficients depend smoothly on ξ_1 and ξ_2.

Case 2: If $c_3 < 0$, following the similar steps of case 1, one can obtain the versal unfold of the perturbed system (17) analogical to system (25). Therefore, if $|\frac{\partial(\mu_1, \mu_2)}{\partial(\xi_1, \xi_2)}|_{\xi_1=\xi_2=0} \neq 0$, the parameter transformations (26) are homeomorphism in a small neighborhood of the origin. By the result in [28], system (6) undergoes Bogdanov-Takens bifurcation of codimension 2 in a small neighborhood of E^* as (ξ_1, ξ_2) varies near the origin. The local expression of the bifurcation curves in a small neighborhood of the origin are

1) saddle-node bifurcation curve
$SN = \{(\xi_1, \xi_2) : \mu_1(\xi_1, \xi_2) = 0, \ \mu_2(\xi_1, \xi_2) \neq 0\}$;

2) Hopf bifurcation curve
$H = \{(\xi_1, \xi_2) : \mu_2(\xi_1, \xi_2) = \pm\sqrt{-\mu_1(\xi_1, \xi_2)}, \ \mu_1(\xi_1, \xi_2) < 0\}$;

3) homoclinic bifurcation curve
$HL = \{(\xi_1, \xi_2) : \mu_2(\xi_1, \xi_2) = \pm\frac{5}{7}\sqrt{-\mu_1(\xi_1, \xi_2)}, \ \mu_1(\xi_1, \xi_2) < 0\}$.

□

Besides, from the expression of c_3 and c_4, we have the following conclusions.

1. If $c_3c_4 > 0$, system (6) undergoes a repelling Bogdanov-Takens bifurcation of codimension 2. Therefore, for some parameters, there exists an unstable limit cycle and unstable homoclinic loop will occur for other parameter values.

2. If $c_3c_4 < 0$, system (6) undergoes an attracting Bogdanov-Takens bifurcation of codimension 2. Therefore, for some parameter values, there exists a stable limit cycle and stable homoclinic loop will occur for other parameter values.

5 Numerical simulations

In this section, we provide numerical simulations to demonstrate the existence of transcritical bifurcation, saddle-node bifurcation, Hopf bifurcation, homoclinic bifurcation and Bogdanov-Takens bifurcation. Bifurcation diagrams, phase portraits and time series are presented under the following conditions

$$\alpha_1 = 0.5,\ \alpha_2 = 1.33578,\ h_2 = 0.2,\ \gamma = 0.2. \tag{27}$$

$$\alpha_1 = 0.078796,\ \alpha_2 = 0.9,\ h_1 = 0.778082,\ \gamma = 0.03. \tag{28}$$

In the bifurcation diagrams, equilibrium is stable (unstable) on the solid (dashed) line. The signs L, B, H and BT represent the saddle-node bifurcation point, transcritical bifurcation point, Hopf bifurcation point and Bogdanov-Takens bifurcation point respectively.

Figure 5 shows transcritical bifurcation and saddle-node bifurcation diagrams of system (6) with respect to the bifurcation parameter h_1 under condition (27). In Figure 5(a) the trivial equilibrium $O(0,0)$ is unstable and interior equilibrium $E_1(0.110959,$
$1.26736)$ is stable when $h_1 < 1$. On the other hand when h_1 crosses the vertical line $h_1 = h_1^{TC} = 1$ to the right, i.e $h_1 > 1 = h_1^{TC}$, the trivial equilibrium $O(0,0)$ becomes stable. At $h_1 = h_1^{TC} = 1$, the trivial equilibrium and interior equilibrium $E_1(0.110959, 1.26736)$ exchanges their stability, and system (6) undergoes transcritical bifurcation. Figure 5(b) displays saddle-node bifurcation diagram around $E_1(0.503967, 0.848173)$ with respect to h_1 for $h_1 = h_1^{SN} = 0.244047$. System (6) has a stable node and saddle point for $h_1 < 0.244097$. At $h_1 = h_1^{SN} = 0.244097$, the stable node and saddle point collide, and disappeared for the parameter $h_1 > h_1^{SN} = 0.244097$. Figure 6 presents saddle-node and Hopf bifurcation diagrams of system (6) with respect to the bifurcation parameter h_2 at $E_1(0.147947, 1.04083)$ and $E_1(0.110953, 1.26739)$ respectively under condition (28). If Hopf bifurcation curve crosses the vertical line $h_2 = 0.0809563$ to the left, system (6) generates an unstable equilibrium point and a stable limit cycle at $h_2 = 0.075$. The phase portrait and the corresponding time diagram of Hopf bifurcation in Figure 6(b) are presented in Figure 7(a) and Figure 7(b) respectively.

Figure 8 is Bogdanov-Takens bifurcation diagram around at $E^*(0.533333, 0.886239)$ in $h_2 - \alpha_2$ parametric space for $\alpha_1 = 0.5, , h_1 = 0.2, \gamma = 0.2$. The red line is Hopf bifurcation curve and the blue line is fold bifurcation curve. Bogdanov-Takens bifurcation is the point of tangency of Hopf bifurcation curve and fold bifurcation curve.

The analytic result in Theorem 4.7 shows the existence of bifurcation curves in a

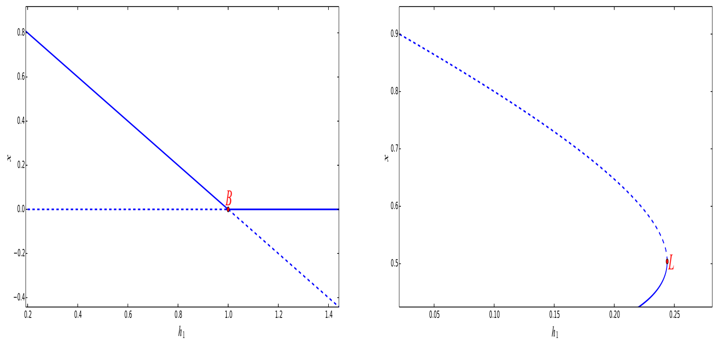

(a) **(b)**

Figure 5: Bifurcation diagrams for system (6) with respect to the bifurcation parameter h_1 under condition (27). **(a)** Transcritical bifurcation at $O(0,0)$ for $h_1 = h_1^{TC} = 1$. **(b)** Saddle-node bifurcation at $E_1(0.503967, 0.848173)$ for $h_1 = h_1^{SN} = 0.244047$.

small neighborhood of the Bogdanov-Takens point which divide the parameter plane into four sub-regions. For $\alpha_1 = 0.5, , h_1 = 0.2, \gamma = 0.2$, the critical values of the bifurcation parameters becomes $\alpha_2^{[BT]} = 2.05441$ and $h_2^{[BT]} = 0.459376$. For small value of ξ_1 and ξ_2, we have

$$\mu_1(\xi_1,\xi_2) = -7.08019\xi_1 + 22.0597\xi_2 + 3.429\xi_1^2 - 21.3674\xi_1\xi_2 + 33.2871\xi_2^2,$$
$$\mu_2(\xi_1,\xi_2) = -2.04556\xi_1 + 4.04788\xi_2 + 0.331097\xi_1^2 - 1.24408\xi_1\xi_2 + 0.662051\xi_2^2,$$

and $\det(\mathrm{J})|_{\xi_1=\xi_2=0} = -20.3795 \neq 0$, where

$$J = \begin{pmatrix} \dfrac{\partial\mu_1}{\partial\xi_1} & \dfrac{\partial\mu_1}{\partial\xi_2} \\ \dfrac{\partial\mu_2}{\partial\xi_1} & \dfrac{\partial\mu_2}{\partial\xi_2} \end{pmatrix}.$$

Moreover,

$$\begin{aligned} c_3 =& 0.671618 + 0.412693\xi_1 - 0.26258\xi_2 - 0.0043378\xi_1^2 + 0.1765\xi_1\xi_2 \\ &- 0.507809\xi_2^2 + 0(\xi^3) > 0, \\ c_4 =& -2.3003 + 0.298929\xi_1 - 0.9314\xi_2 + 0.172809\xi_1^2 - 0.66762\xi_1\xi_2 \\ &+ 0.402549\xi_2^2 + 0(\xi^3) < 0. \end{aligned}$$

Therefore, system (6) undergoes attracting Bogdanov-Taken bifurcation of codimension 2. The local representations of the bifurcation curves up to second-order approximations are

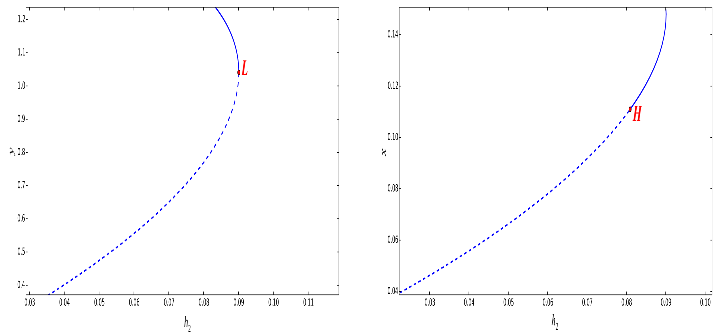

(a) **(b)**

Figure 6: Bifurcation diagrams for system (6) with respect to the bifurcation parameter h_2 under condition (28). **(a)** Saddle-node bifurcation at $E_1(0.147947, 1.04083)$ for $h_2 = h_2^{SN} = 0.0900955$. **(b)** Hopf bifurcation at $E_1(0.110953, 1.26739)$ for $h_2 = h_2^* = 0.0809563$.

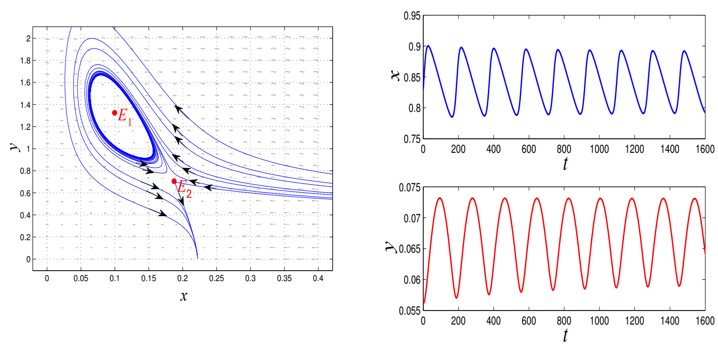

(a) **(b)**

Figure 7: Phase portrait and corresponding time series for Figure 6(b) . **(a)** Phase portrait of the stable limit cycle created by supercritical Hopf bifurcation. **(b)** Time series of the stable limit cycle

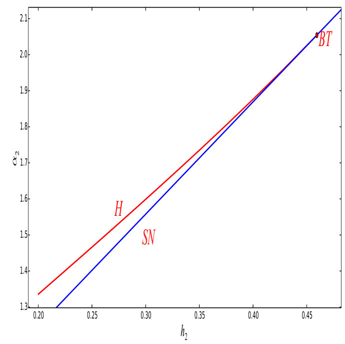

Figure 8: Bogdanov-Takens bifurcation diagram of system (6) at $E^*(0.533333, 0.886239)$ in $h_2 - \alpha_2$ plane for $\alpha_1 = 0.5$, , $h_1 = 0.2$, $\gamma = 0.2$.

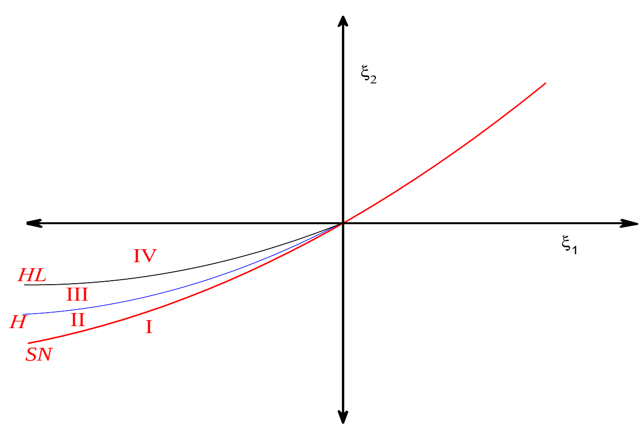

Figure 9: Attracting Bogdanov-Takens bifurcation diagram of system (17) in $\xi_1 - \xi_2$ plane.

1) saddle-node bifurcation curve
$SN = \{(\xi_1, \xi_2) : -7.08019\xi_1 + 22.0597\xi_2 + 3.429\xi_1^2 - 21.3674\xi_1\xi_2 + 33.2871\xi_2^2 = 0,\ \mu_2 \neq 0\}$;

2) Hopf bifurcation curve
$H = \{(\xi_1, \xi_2) : -7.08019\xi_1 + 22.0597\xi_2 + 7.61333\xi_1^2 - 37.9278\xi_1\xi_2 + 49.6724\xi_2^2 = 0,\ \mu_1 < 0\}$;

3) homoclinic bifurcation curve
$HL = \{(\xi_1, \xi_2) : -3.61234\xi_1 + 11.2549\xi_2 + 5.93382\xi_1^2 - 27.4621\xi_1\xi_2 + 33.3685\xi_2^2 = 0,\ \mu_1 < 0\}$.

Figure 9 is the sketch of the bifurcation curves. The red curve, blue curve and black curve represent the saddle-node bifurcation, Hopf bifurcation and homoclinic bifurcation curve respectively. These curves divide the neighborhood of the origin into four regions. The phase portraits in each region are displayed in Figure 10. For $(\xi_1, \xi_2) = (0, 0)$, the unique interior equilibrium is a cusp of codimension 2 (see Figure 10(a)). In region I, there is no interior equilibrium (see Figure 10(b)), and both species will tend to extinction for all initial values. There is a unique interior equilibrium (a saddle-node) on the saddle-node bifurcation curve SN. Moving clockwise across the saddle-node SN curve into region II, a stable hyperbolic focus and a hyperbolic saddle appear (see Figure 10(c)). There are two interior equilibria on the Hopf bifurcation curve: a stable focus and a hyperbolic saddle. If the parameters cross the Hopf bifurcation curve into region III, a stable limit cycle enclosing an unstable hyperbolic focus will appear through the supercritical Hopf bifurcation, and hyperbolic saddle also exists (see Figure 10(d)). If the parameter leave region III and lie on homoclinic bifurcation curve HL, a stable homoclinic loop enclosing an unstable hyperbolic focus will occur through the homoclinic bifurcation (see Figure 10(e)). Finally, in region IV, an unstable hyperbolic focus and a saddle point appear (see Figure 10(f)).

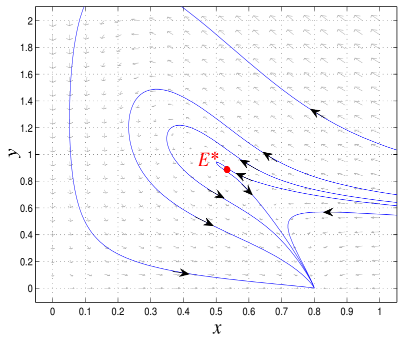

(a) $\xi_1 = 0$ & $\xi_2 = 0$.

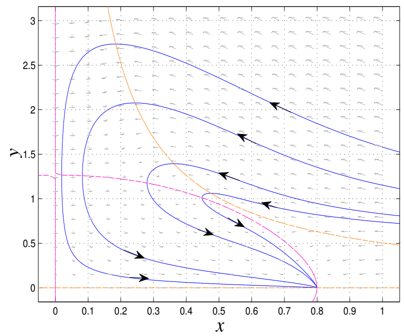

(b) $\xi_1 = -0.306$ & $\xi_2 = -0.073$.

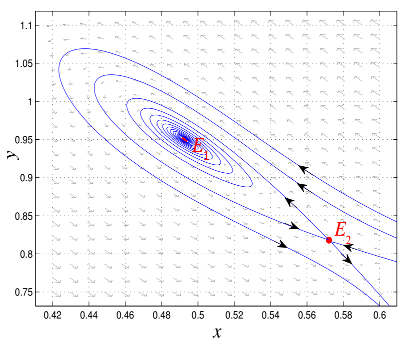

(c) $\xi_1 = -0.3065$ & $\xi_2 = -0.102$.

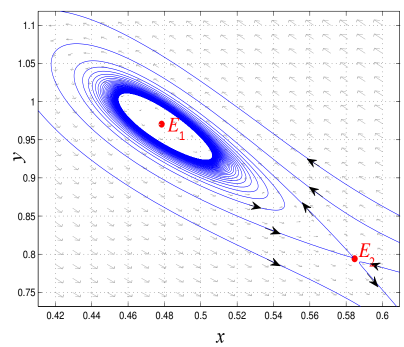

(d) $\xi_1 = -0.306$ & $\xi_2 = -0.105$.

Figure 10: Phase portraits of the perturbed system (17). **(a)** A cusp of codimension 2. **(b)** No interior equilibria in the region I. **(c)** Stable hyperbolic focus and saddle point in the region II. **(d)** Unique and stable limit cycle enclosing unstable hyperbolic focus and saddle point in the region III.

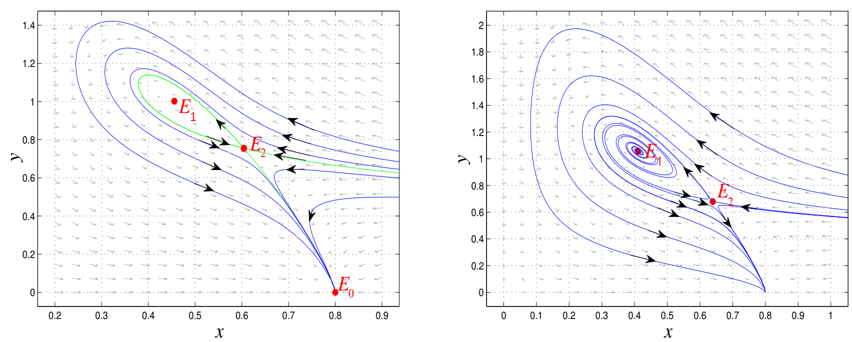

(e) $\xi_1 = -0.306$ & $\xi_2 = -0.1116$ **(f)** $\xi_1 = -0.306$ & $\xi_2 = -0.13$.

Figure 10: Continued figures
(e) Stable homoclinic loop enclosing unstable hyperbolic focus $E_1(0.45543, 1.008)$.
(f) Unstable hyperbolic focus and a saddle point in the region VI.

6 Conclusion

In this paper, we studied the dynamics of a predator-prey model with Cosner type functional response and combined harvesting. The analysis reveals that harvesting of both the prey and the predator species play an important role in determining the dynamics and bifurcations of the model. In comparison to the model with no or constant prey harvesting, our model generates many novel dynamical behaviors. For example, the trivial boundary equilibrium $O(0,0)$, which was a hyperbolic saddle in the original model (model with no harvesting) and did not exist in the constant prey harvesting model, appears to be a locally asymptotically stable equilibrium in our model. The point that occurred in the original model, a high consumption rate caused the extinction of the predators, does not occur in the new model.

The model also exhibits different types of codimension one and codimension two bifurcations including transcritical bifurcation, saddle-node bifurcation, Hopf bifurcation, homoclinic bifurcation and Bogdanov–Takens bifurcation. It presents steady-state behavior, limit cycle, homoclinic loop, and the extinction of one or both species in close proximity to the BT point. If the limit cycle collides with a saddle point, a homoclinic loop is formed. In that case, the oscillation of population density of both species becomes maximal, i.e., the system has the big limit cycle on the homoclinic bifurcation line. On one side of the homoclinic bifurcation line, all species survive, while on the other, one or both species may become extinct.

Acknowledgments

The authors would like to acknowledge the financial support from the NSFC (No. 52071298), ZhongYuan Science and Technology Innovation Leadership Program (No. 214200510010), the Training Plan for Young Backbone Teachers of Henan University of Technology, the Innovative Funds Plan of Henan University of Technology (2020ZKCJ09).

Author contributions

B. M. and L. Y. formulated the model and analyzed it, B. M. wrote the manuscript, J. R., L. Y. and Q. Y. critically reviewed and edited the manuscript, J. R. supervised the project. Finally, all authors read and approved the final manuscript.

Conflict of interest

The authors have no any conflict of interest.

Availability of data and materials

All computational data are included in the article.

Competing interests

The authors have no relevant financial or non-financial interest to disclose.

Ethics approval and consent to participate

Not applicable.

Consent for publication

All the authors have agreed and given their consent for the publication of this research paper.

References

[1] A. J. Lotka, Elements of Physical Biology, first ed., Williams and Wilkins, Baltimore, 1925.

[2] V. Volterra, Fluctuations in the abundance of a species considered mathematically, Nature **118** (1926) 558-560. 10.1038/118558a0.

[3] B. T. Mulugeta, L. P. Yu, J. L. Ren, Bifurcation analysis of a one-prey and two-predators model with additional food and harvesting subject to toxicity, Int. J. Bifurc. Chaos Appl. Sci. Eng. **31** (2021) 2150089. https://doi.org/10.1142/S0218127421500899.

[4] D. M. Xiao S. G. Ruan, Global analysis in a predator-prey system with non-monotonic functional response, SIAM J. Appl. Math. **61** (2001) 1445-1472. DOI:10.1137/s0036139999361896.

[5] J. C. Huang, S. G. Ruan, S. Song, Bifurcations in a predator-prey system of Leslie type with generalized Holling type III functional response, J. Differ. Equ. **257** (2014) 1721-1752. DOI:10.1016/j.jde.2014.04.024.

[6] M. Haque, A detailed study of the Beddington-DeAngelis predator-prey model, Math. Biosci. **234** (2001) 1-16. DOI:10.1016/j.mbs.2011.07.003.

[7] D. M. Xiao, S. G. Ruan, Global dynamics of a ratio-dependent predator-prey system, J. Math. Biol. **43** (2001) 268-290. DOI:10.1007/s002850100097.

[8] D. M. Xiao, W. X. Li, M. Han, Dynamics in a ratio-dependent predator-prey model with predator harvesting, J. Math. Anal. Appl. **324** (2006) 14-29. DOI:10.1016/j.jmaa.2005.11.048.

[9] S. N. Raw, P. Mishra, R. Kumar, S. Thakur, Complex behavior of prey-predator system exhibiting group defense: A mathematical modeling study, Chaos Solitons Fract. **100** (2017) 74-90. DOI:10.1016/j.chaos.2017.05.010.

[10] S. Sirisubtawee, N. Khansai, A. Charoenloedmongkhon, Investigation on dynamics of an impulsive predator-prey system with generalized Holling type IV functional response and anti-predator behavior, Adv. Differ. Equ. **2021** (2021) 1-26. https://doi.org/10.1186/s13662-021-03324-w.

[11] C. Cosner, D. L. DeAngelis, J. S. Ault, D. B. Olson, Effects of spatial grouping on the functional response of predators, Theor. Popul. Biol. **56** (1999) 65-75. DOI:10.1006/tpbi.1999.1414.

[12] K. Ryu, W. Ko, H. Haque, Bifurcation analysis in a predator-prey system with a functional response increasing in both predator and prey densities, Nonlinear Dyn. **94** (2018) 1639-1656. DOI:10.1007/s11071-018-4446-0.

[13] B. Tiwari, S. N. Raw, P. Mishra, Qualitative analysis of a spatiotemporal prey-predator model with multiple Allee effect and schooling behavior, Nonlinear Dyn. **102** (2020) 3013-3038. https://doi.org/10.1007/s11071-020-06018-2.

[14] J. F. Luo, Y. Zhao, Stability and bifurcation analysis in a predator–prey system with constant harvesting and prey group defense, Int. J. Bifurc. Chaos Appl. Sci. Eng. **27** (2017) 1750179. DOI:10.1142/S0218127417501796.

[15] M. Sen, P. D. N. Srinivasu, M. Banerjee, Global dynamics of an additional food provided predator–prey system with constant harvest in predators, Appl. Math. Comput. **250** (2015) 193-211. DOI:10.1016/j.amc.2014.10.085.

[16] L. F. Cheng, L. T. Zhang, Bogdanov–Takens bifurcation of a Holling IV prey-predator model with constant-effort harvesting, J. Inequalities Appl. **1** (2021) 1-23. https://doi.org/10.1186/s13660-021-02597-9.

[17] A. Rojas-Palma, E. González-Olivares, Optimal harvesting in a predator-prey model with Allee effect and sigmoid functional response, Appl. Math. Modell. **36** (2012) 1864-1874. DOI:10.1016/j.apm.2011.07.081.

[18] X. X. Liu, Q. D. Huang, The dynamics of a harvested predator–prey system with Holling type IV functional response, Biosystems **169** (2018) 26-39. DOI:10.1016/j.biosystems.2018.05.005.

[19] R. P. Gupta, P. Chandra, M. Banerjee, Dynamical complexity of a prey-predator model with nonlinear predator harvesting, Discrete Contin. Dyn. Syst.-B **20** (2015) 422-443. doi:10.3934/dcdsb.2015.20.423.

[20] M. G. Mortuja, M. K. Chaube, S. Kumar, Dynamic analysis of a predator-prey system with nonlinear prey harvesting and square root functional response, Chaos Solitons Fract. **148** (2021) 111071. doi.org/10.1016/j.chaos.2021.111071.

[21] S. Kumar, H. Kharbanda, Chaotic behavior of predator-prey model with group defense and non-linear harvesting in prey, Chaos Solitons Fract. **119** (2019) 19-28. DOI:10.1016/j.chaos.2018.12.011.

[22] D. P. Hu, H. J. Cao, Stability and bifurcation analysis in a predator–prey system with Michaelis–Menten type predator harvesting, Nonlinear Anal. Real world Appl. **33** (2017) 58-82. DOI:10.1016/j.nonrwa.2016.05.010.

[23] H. Fattahpour, W. Nagata, H. R. Zangeneh, Prey–predator dynamics with two predator types and Michaelis–Menten predator harvesting, Differ. Equ. Dyn. Syst. (2019) 1-26. DOI:10.1007/s12591-019-00500-z.

[24] W. C. Chen, Stability and bifurcation analysis of a predator-prey model with Michaelis-Menten type prey harvesting, J. Appl. Math. Phys. **10** (2022) 504-526. https://doi.org/10.4236/jamp.2022.102038.

[25] U. Ghosh, P. Majumdar, J. K. Ghosh, Bifurcation analysis of a two-dimensional predator–prey model with Holling type IV functional response and nonlinear predator harvesting, J. Biol. Syst. **28** (2020) 839-864. https://doi.org/10.1142/S0218339020500199.

[26] Z. C. Shang, Y. H. Qiao, L. J. Duan, J. Miao, Bifurcation analysis in a predator–prey system with an increasing functional response and constant-yield prey harvesting, Math. Comput. Simulation **190** (2021) 976-1002. https://doi.org/10.1016/j.matcom.2021.06.024.

[27] Z. F. Zhang, T. R. Ding, W. Z. Huang, Z. X. Dong, Qualitative Theory of Differential Equation, Translations of Mathematical Monographs, **101**, American Mathematical Society, Providence, Rhode Island, 1992.

[28] L. Perko, Differential Equations and Dynamical Systems, third ed., Springer-Verlag, New York, 2001.